Novel Broadband Planar Reflectarray With Parasitic Dipoles for Wireless Communication Applications

Long Li, *Member, IEEE*, Qiang Chen, *Member, IEEE*, Qiaowei Yuan, Kunio Sawaya, *Senior Member, IEEE*, Tamami Maruyama, *Member, IEEE*, Tatsuo Furuno, *Member, IEEE*, and Shinji Uebayashi, *Member, IEEE*

***Abstract*—A novel broadband planar reflectarray with parasitic dipoles is presented for wireless communication applications. A unit cell of the microstrip reflectarray consists of a printed main dipole with a pair of parasitic dipoles. The introduction of parasitic dipoles can effectively extend the reflection phase range beyond 360°, which overcomes the problem of an inadequate phase range when using thicker substrates for a wider operational bandwidth. The parasitic dipole reflectarrray (PDR) is applied to a wideband CDMA (WCDMA) system to eliminate blind spots in communication between the base station and mobile users. A practical link budget analysis demonstrates the effectiveness of the proposed planar reflectarray.**

***Index Terms*—Parasitic dipole reflectarray (PDR), reflection phase, blindness, link budget analysis, wideband CDMA (WCDMA).**

I. Introduction

A MICROSTRIP reflectarray is a flat, low-profile reflector consisting of an array of microstrip patch elements, and it reflects a beam in a specified direction when illuminated by a primary source. The planar reflectarray is rapidly becoming an attractive alternative to the conventional parabolic reflector antenna because of its advantages, such as that it can be surface-mounted due to low mass and volume, it can be easily deployed, it has a low manufacturing cost, it has a scannable beam, and it can be integrated with a solar array [1]–[3]. In wireless communication scenarios such as that involving a large-scale outdoor/indoor base station in a wireless local area network (WLAN) system, planar reflectarray antennas can be mounted on the ceiling or embedded into walls to reflect beams in order to cover different areas, especially the blind areas for the primary source.

The reflectarray is based on the phase compensating for the dimensions of each element in the array in order to generate cophase reradiation and to concentrate it toward a specific direction. Many phasing schemes have recently been developed that involve all identical microstrip patch elements but with different-length delay lines [1], [2], microstrip patches or dipoles with varying dimensions [3]–[5] or identical patches with different angular rotation [6]. To achieve a wider bandwidth for a conventional reflectarray, some techniques have been proposed, such as employing a thick substrate and stacking multiple patches [7], [8]. However, multilayer configurations are very costly and incur serious surface-wave losses at millimeter-wave frequencies. The results of a single dipole element have demonstrated that a larger operational bandwidth can be achieved using thicker substrates at the expense of an inadequate phase range of less than 360° [9]. This inadequate phase range leads to reflectarray element phase errors that consequently reduce the directivity of the reflectarray.

In this letter, a novel broadband planar reflectarray with parasitic dipoles is presented for wireless communication applications. The unit cell of the microstrip reflectarray is composed of a main dipole with a pair of parasitic dipoles printed on a single-layer substrate. Two degrees of freedom are introduced to extend the phase range of the unit cell to more than 360°: the ratio of the length of the parasitic dipoles to that of the main dipole and the distance between the main dipole and parasitic dipoles. The new unit cell is capable of offering a phase range that well exceeds 360° for a broadband reflectarray design using thicker substrates. Furthermore, a parasitic dipole reflectarray (PDR) with a large scan angle is designed and applied to a wideband CDMA (WCDMA) system to eliminate blind spots in communication between the base station and mobile users. A practical link budget analysis demonstrates the effectiveness of the proposed planar reflectarray.

II. Analysis and Design of Parasitic Dipole Reflectarray

The new unit cell consists of a main dipole and a pair of parasitic dipoles printed on a single-layer substrate as shown in Fig. 1(a). The center dipole is called the main dipole and has length l_m and width w_m. The other two dipoles are positioned symmetrically on the sides of the main dipole. These two dipoles have the same length, l_p, and width, w_p. For simplicity of the reflectarray design, the dimensions of the two dipoles are dependent on those of the main dipole. This is why they are called parasitic dipoles in this letter. Only two degrees of freedom are introduced, which are ratio r of the length of the parasitic dipoles to that of the main dipole $(l_p/l_m = r)$ and distance d between the main dipole and parasitic dipoles.

An infinite periodic model using the HFSS simulation [10] was performed to analyze the reflection phase characteristics of the parasitic dipole element, as shown in Fig. 1(b). In the model used to calculate the reflection phase of the incident plane wave, the reflection plane (observation plane) was set in the

Manuscript received April 18, 2009; revised June 08, 2009, July 03, 2009. First published July 24, 2009; current version published August 18, 2009.

L. Li is with School of Electronic Engineering, Xidian University, Xi'an 710071, China (e-mail: lilong@mail.xidian.edu.cn, lilong@ecei.tohoku.ac.jp).

Q. Chen and K. Sawaya are with the Department of Electrical and Communication Engineering, Tohoku University, Sendai 980-8579, Japan (e-mail: chenq@ecei.tohoku.ac.jp; sawaya@ecei.tohoku.ac.jp).

Q. W. Yuan was with Tohoku University, Sendai 980-8579, Japan. She is now with Sendai National College of Technology, Sendai 989-3128, Japan (e-mail: qwyuan@cc.sendai-ct.ac.jp; qwyuan@ecei.tohoku.ac.jp).

T. Maruyama, T. Furuno, and S. Uebayashi are with NTT DOCOMO, Kanagawa 239-8536, Japan (e-mail: maruyamatam@nttdocomo.co.jp; furuno@nttdocomo.co.jp; uebayashi@nttdocomo.co.jp).

Color versions of one or more of the figures in this letter are available online at http://ieeexplore.ieee.org.

Digital Object Identifier 10.1109/LAWP.2009.2028298

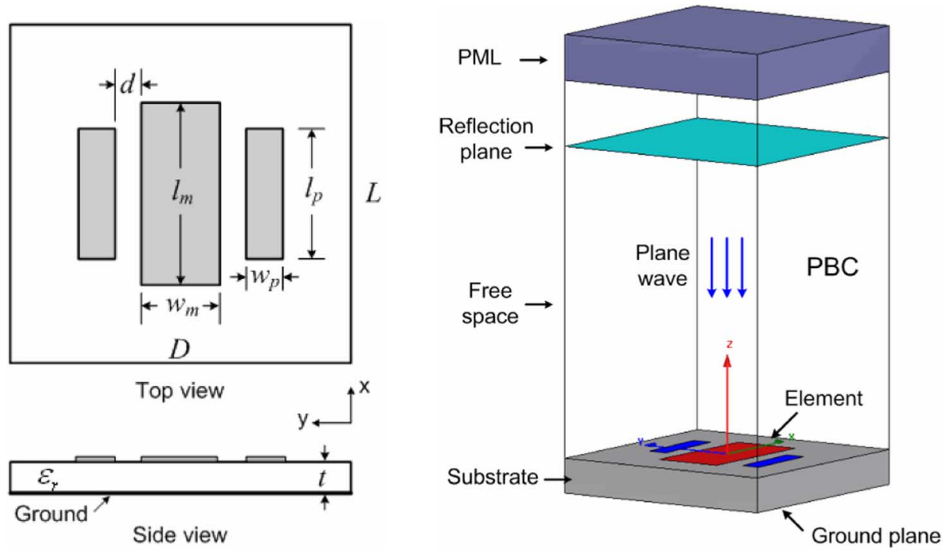

(a) (b)

Fig. 1. (a) Geometry of parasitic dipole element. (b) An infinite periodic model based on finite element algorithm used to calculate the reflection phase of a plane wave that is normally incident in which periodic boundary conditions (PBC) are in place around the unit cell.

far-field zone of the unit cell surface. A perfectly matched layer (PML) was positioned to absorb the reflected waves. The scattered E-field on the observational plane was recorded, and the reflection phase on this plane was calculated using

$$\phi_{\text{unit cell}} = \frac{\int_S \text{Phase}(E_{\text{scattered}})ds}{\int_S \hat{s} \cdot d\overrightarrow{s}} + \frac{2\pi}{\lambda}h \qquad (1)$$

where S is the evaluated reflection plane and $\hat{s}$ is its normal unit vector. The scattered E-field data from a projected incident wave is directly available as an input to the Field Calculator following the nominal HFSS simulation [10]. Term h is the distance between the reflection plane and the surface of parasitic dipole element. Term λ is the operating wavelength. The period of the unit cell is $L = D = 5$ mm. The substrate thickness is $t = 0.76$ mm, and the permittivity is $\varepsilon_r = 2.5$. The width of the main dipole is $w_m = 2w_p = 1$ mm. The operational frequency is 24 GHz.

Fig. 2 shows the reflection phase of the unit cell versus the length of the main dipole when the plane wave is incident normal to the surface. The figure shows first that the current calculation results for a single main dipole agree well with the results obtained by Pilz and Menzel using spectral domain techniques [4]. Second, compared to the reflection phase of a single dipole, the introduction of parasitic dipoles extends the phase range beyond 360°. Third, even if the substrate thickness is 1.5 mm, the phase range is still exceeds 500°. This is due to the multiresonance response and mutual coupling between the main dipole and parasitic dipoles. A similar analysis was reported in [11], which showed that the phase range can be extended by utilizing resonant elements that are similar in shape but different in size. Here the symmetric configuration of the parasitic dipoles is convenient for the design of the PDR. Furthermore, Fig. 3 shows how the phase range varies with two degrees of freedom, namely r and d. The figure shows that the new unit cell is capable of offering a phase range that well

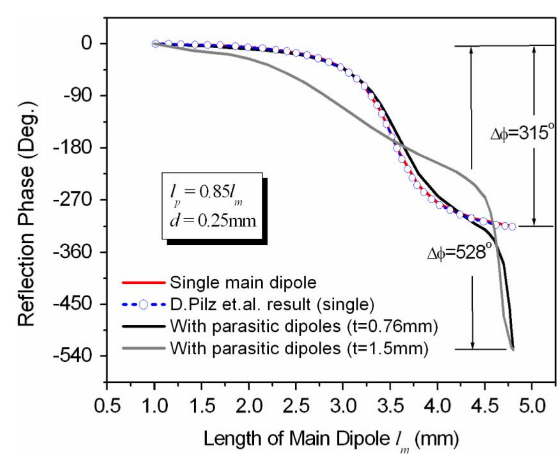

Fig. 2. Reflection phase characteristics versus the length of main dipole.

exceeds 360° and has a slower slope (smaller gradient) of the reflected wave phase for a broadband reflectarray design.

The key technique in the design of a reflectarray is how to design the individual elements so that they scatter the incident wave with the proper phase compensation to produce a beam toward a specific direction. The configuration of a standard microstrip reflectarray is shown in Fig. 4. The reradiated field from the dipoles in an arbitrary direction, $\hat{u}$, will be in the form of [1]

$$E(\hat{u}) = \sum_{m=1}^{M}\sum_{n=1}^{N} F(\overrightarrow{r}_{mn} \cdot \overrightarrow{r}_f) A(\overrightarrow{r}_{mn} \cdot \hat{u}_0) A(\hat{u} \cdot \hat{u}_0) \cdot \exp\{-jk_0[|\overrightarrow{r}_{mn} - \overrightarrow{r}_f| + \overrightarrow{r}_{mn} \cdot \hat{u}] + j\phi_{mn}\} \qquad (2)$$

where F is the feed pattern function, A is the pattern function of the parasitic dipole elements. Terms $\overrightarrow{r}_{mn}$ and $\overrightarrow{r}_f$ are the position vectors of the mnth element and the feed horn antenna, respectively. Term $\hat{u}_0$ is the desired main-beam pointing direction of the reflectarray. Phase ϕ_{mn} is the required phase of the scattered field from the mnth element. The condition for an array

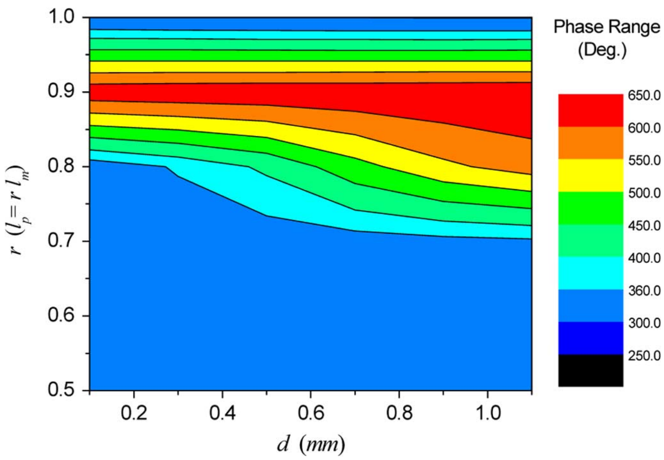

Fig. 3. Reflection phase range versus r and d of the parasitic dipole cell ($l_p = rl_m, w_m = 2w_p = 1.0$ mm, $L = D = 5.0$ mm, $t = 0.76$ mm, $\varepsilon_r = 2.5$, and $f = 24$ GHz).

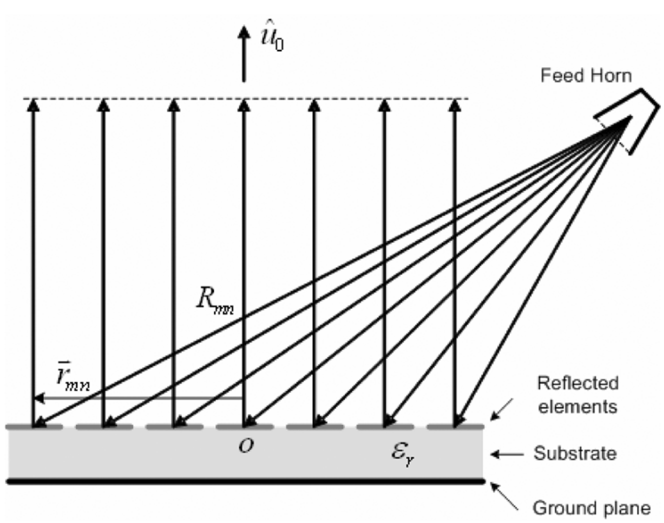

Fig. 4. Configuration of microstrip reflectarray.

aperture distribution to be cophase in the desired direction, $\hat{u}_0$, is given by

$$\phi_{mn} - k_0(R_{mn} + \vec{r}_{mn} \cdot \hat{u}_0) = 2p\pi, \quad p = 0, \pm 1, \pm 2, \ldots \tag{3}$$

where R_{mn} is the distance from the feed source to the mnth array element, i.e., $R_{mn} = |\,\vec{r}_{mn} - \vec{r}_f\,|$.

According to the differential phase curve shown in Fig. 2, the resonant length of the mnth element is determined to produce a phase shift, ϕ_{mn}, in the field scattered from the parasitic dipole element.

III. Link Budget Analysis in WCDMA System

In wideband wireless communications for mobile users, it is a significant problem to eliminate the blind spots of base station antennas in a downtown, high-building district. Generally, some RF boosters are used to extend the cellular coverage area, but standard RF boosters need transceivers, power supplies, cables, etc., which have a high cost and are limited in terms of installation space. In this letter, a planar reflectarray is used as a reflector that is set on the top of a building or embedded into a wall. Through proper designs, the reflectarray can steer the main beam to cover the blind spots of base station antennas, as shown in Fig. 5. The merits of an erect installation are not only that quake-resistance standards can be taken into account, but also that the reflectarray can be integrated with some types of advertisement boards. However, if a metallic reflector is employed, it is very difficult to control the reflected beam in a specified direction.

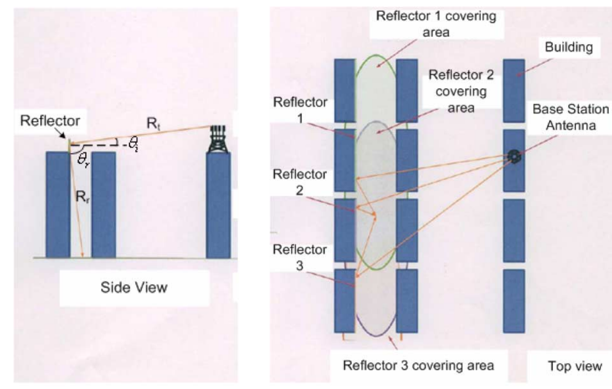

(a) (b)

Fig. 5. Elimination of blindness using reflectarrays in wireless communication system, (a) side view, (b) top view.

A PDR was designed and applied to a WCDMA system. The WCDMA (Rel.99) system requires paired spectra: one band (1920–1980 MHz) for the uplink and one (2110–2170 MHz) for the downlink [12]. Here, the central operating frequency of the PDR is set to 2050 MHz, and more than 10% of its bandwidth is required to cover both the uplink and downlink spectra. Considering the wireless communication system model shown in Fig. 5, we designed a 60°-beam-steering PDR, which means that for the downlink, a plane wave is propagated from a base station antenna that is normally incident to the PDR, and the reflected main beam is steered in the direction of 60°. For the uplink, a plane wave from a mobile user is incident at an oblique angle of 60° to the PDR, and the reflected main beam is required to be normal. Fig. 6 shows the reflection phase curve of the parasitic dipole element operating at 2050 MHz. It can be seen from Fig. 6(b) that the reflection phase curves are not greatly affected by the incidence angles, even when the incidence angle is greater than 45°. Thus, a PDR with 11×5 elements was simply designed based on the reflection phase characteristics of a plane wave that is normal incident.

The geometry of the designed parasitic dipole reflectarray is shown in Fig. 7 in rows and columns. The reflectarray parameters and the relation between the main dipoles and parasitic dipoles are shown in Fig. 6(a). Since the main beam is scanned only in the *xoz* plane, the dimensions of main dipoles within each column are the same. Table I gives the dimension of main dipoles in each column and the required compensation phases.

Fig. 8(a) shows the radiation patterns of the PDR for the downlink and uplink in the *xoz* plane. In the downlink, the plane wave is incident normal to the reflectarray, i.e., $(\theta_i, \phi_i) = (0°, 0°)$, and the reflected main beam is directed to $(\theta_r, \phi_r) = (60°, 0°)$, but the main beam is reflected inversely for the uplink. The incident E-field is theta polarization. Fig. 8(a) shows that the designed PDR satisfies the requirements on the main beam position very well. Fig. 8(b) shows the

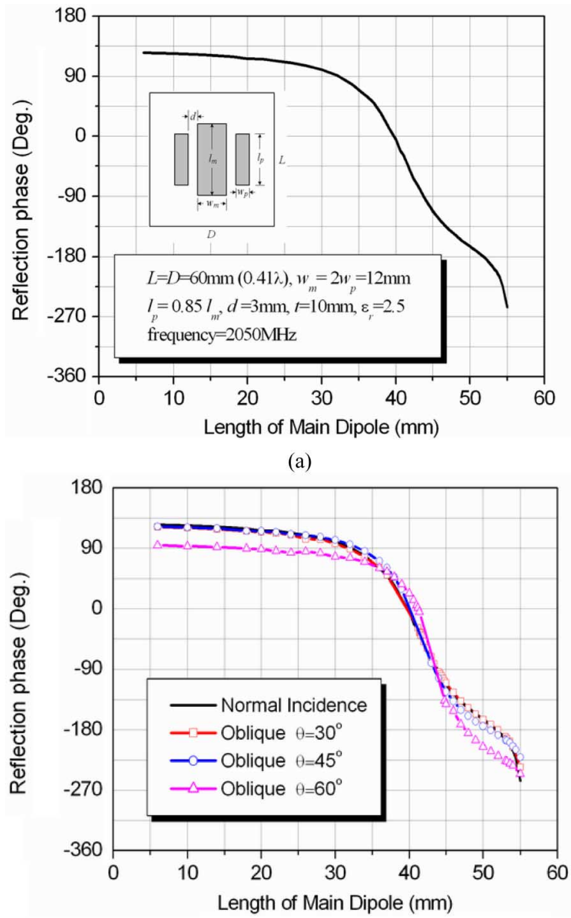

(a)

(b)

Fig. 6. Reflection phase versus main dipole length for a PDR operating at 2050 MHz with (a) plane wave normal incidence and (b) plane wave incidence at various angles.

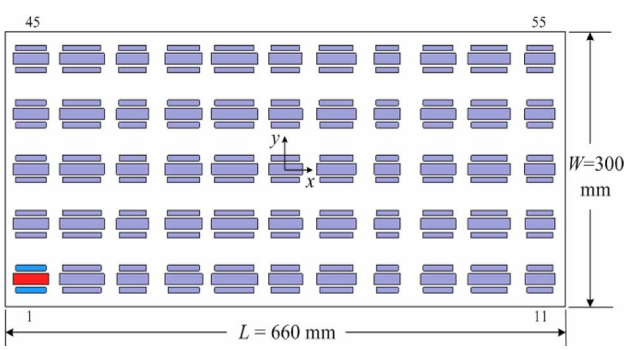

Fig. 7. A parasitic dipole reflectarray of 11 × 5 elements.

TABLE I
MAIN DIPOLES DIMENSIONS AND COMPENSATION PHASE FOR EACH ELEMENT

Column	Dimension of main dipoles (mm)	Compensation phase (Deg.)
1	42.38	-62.42
2	52.98	166.06
3	37.97	34.54
4	44.10	-96.97
5	55.48	131.51
6	39.70	0.00
7	46.51	-131.51
8	30.76	96.97
9	41.30	-34.53
10	50.22	-166.04
11	35.82	62.45

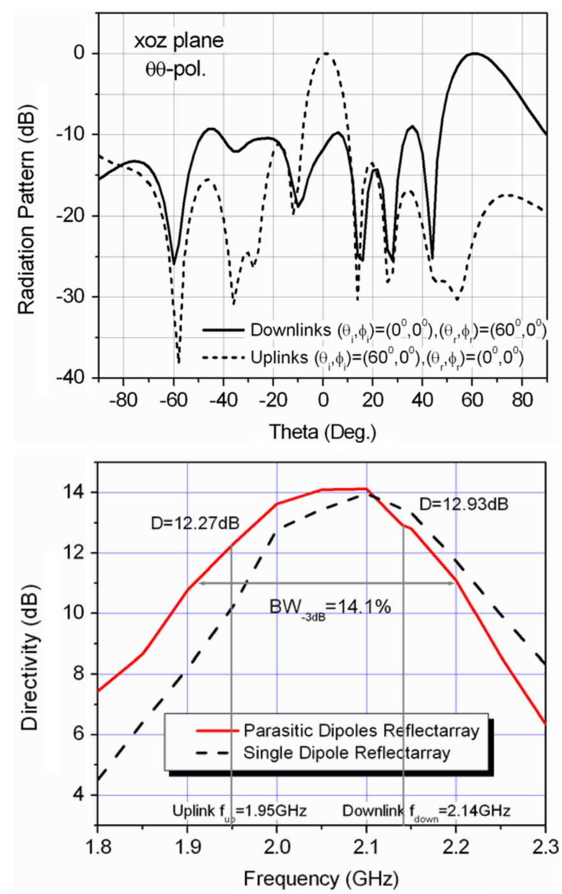

(b)

Fig. 8. (a) Radiation patterns of the reflectarray for downlink and uplink. (b) Comparison of directivity versus frequency of the parasitic dipoles reflectarray and single dipole reflectarray.

computed directivity against frequency. The maximum directivity of the PDR is 14.2 dB. The directivity of the reflectarray is defined as the ratio of the scattered intensity in the main beam direction from the reflectarray to the scattered intensity averaged over all directions. As shown in Fig. 8(b), the −3-dB directivity-drop bandwidth of 14.1% is achieved to cover the uplink and downlink spectra. For comparison, the reflectarray using only a single printed dipole on the same substrate was designed and analyzed. Represented as the dashed line in Fig. 8(b), the maximum directivity (13.9 dB) and the bandwidth $(\mathrm{BW}_{-3\ \mathrm{dB}} = 12.3\%)$ of the single printed dipole are less than those for the PDR. This is because the inadequate phase range of the single dipole reflectarray leads to element phase error, which in turn decreases its directivity and bandwidth.

To demonstrate the elimination of blindness using the reflectarray in the wireless communication system model shown in Fig. 5, we give a simple link budget analysis for the WCDMA (Rel.99) system. Considering the radar range equation

$$P_r = \left(\frac{P_t G_t}{4\pi R_t^2}\right) \cdot \left(\frac{\sigma}{4\pi R_r^2}\right) \cdot \left(\frac{G_r \lambda^2}{4\pi}\right) \quad (4)$$

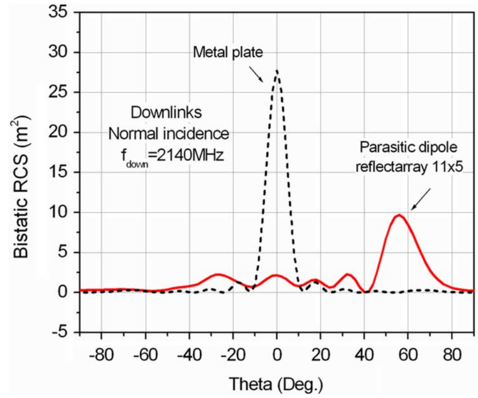

Fig. 9. Bistatic RCS of a parasitic dipole reflectarray and a metal plate with the same dimension for downlinks at 2140 MHz.

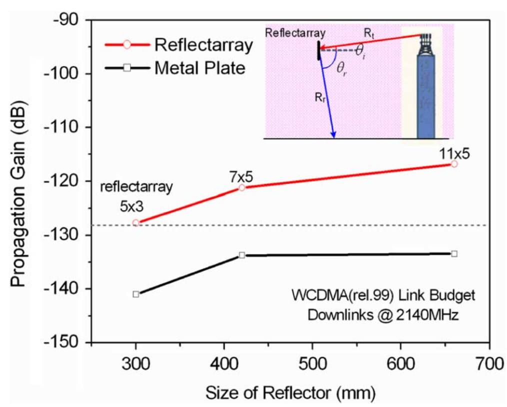

Fig. 10. Link budget analysis of propagation gain in WCDMA (Rel. 99) system using various reflectors.

the first term represents the power density incident to the reflectarray, the second term represents the scattering power density at the receiver from the reflectarray, and the third term denotes the effective area of the receiving antenna. Term σ is the bistatic radar cross section (RCS) of the reflectarray. The bistatic RCS of the PDR working at 2140 MHz for the downlink is shown in Fig. 9. For comparison, the bistatic RCS of a metal plate with the same dimensions as the reflectarray is also given in Fig. 9.

Considering conventional cellular mobile communications, we assume the maximum R_t and R_r are 500 and 40 m, respectively. Generally, the transmitter and receiver antenna gains are 10 and 0 dBi, respectively. Therefore, we can predict the minimum propagation gain $(\mathrm{PG} = P_r/P_t)$ [12] using various reflectors, as shown in Fig. 10. The dashed line shown in Fig. 10 represents the threshold of the propagation gain. Blindness would occur if the propagation gains were less than -128 dB. The results show that if we use a PDR with 11×5 elements, the signal propagation gain can be improved effectively, which successfully eliminates the blindness in the original communication environment. However, if a metal plate is used as the reflector, it does not work even if the size of the plate is increased. Similar conclusions for the uplink can be drawn, which demonstrate the effectiveness of the proposed reflectarray.

IV. Conclusion

This letter proposed a new unit cell for a broadband planar reflectarray design, which consists of a main dipole with a pair of parasitic dipoles printed on a single-layer substrate. The new unit cell is capable of offering a phase range that well exceeds 360° for a wider operational bandwidth of the reflectarray. To achieve a simple design of the planar reflectarray, only two degrees of freedom, namely r and d, are introduced in this letter. It is worthwhile to point out that there is greater potential to obtain a wider bandwidth if the parasitic dipoles are set free from the main dipole. This is because more degrees of freedom can be utilized in that case, but the design complexity of the reflectarray will also increase greatly. In this study, a parasitic dipole reflectarray was implemented into a WCDMA system and was designed to eliminate the blindness in wireless mobile communications. A link budget analysis demonstrated the effectiveness of the proposed reflectarray.

Acknowledgment

The authors gratefully acknowledge the helpful comments and suggestions provided by reviewers and editors.

References

[1] J. Huang, "Analysis of a microstrip reflectarray antenna for microspacecraft applications," TDA Progress Report 42-120, Feb. 1995, pp. 153–173.
[2] D. C. Chang and M. C. Huang, "Multiple-polarization microstrip reflectarray antenna with high efficiency and low cross-polarization," *IEEE Trans. Antennas Propag.*, vol. 43, no. 8, pp. 829–834, Aug. 1995.
[3] S. D. Targonski and D. M. Pozar, "Analysis and design of a microstrip reflectarray using patches of variable size," in *Proc. IEEE AP-S/URSI Int. Symp. Dig.*, Seattle, WA, Jun. 20–24, 1994, pp. 1820–1823.
[4] D. Pilz and W. Menzel, "Full wave analysis of a planar reflector antenna," in *Proc. Asia-Pacific Microw. Conf.*, Dec. 2–5, 1997, pp. 225–227.
[5] L. Li, Q. Chen, Q. W. Yuan, K. Sawaya, T. Maruyama, T. Furuno, and S. Uebayashi, "Microstrip reflectarray using crossed-dipole with frequency selective surface of loops," in *Proc. ISAP*, Taipei, Taiwan, Oct. 27–30, 2008, no. 1645278.
[6] J. Huang and R. J. Pogorzelski, "A Ka-band microstrip reflectarray with elements having variable rotation angles," *IEEE Trans. Antennas Propag.*, vol. 46, no. 5, pp. 650–656, May 1998.
[7] D. M. Pozar, T. S. Targonsky, and H. D. Syrigos, "Design of millimeter wave microstrip reflectarrays," *IEEE Trans. Antennas Propag.*, vol. 45, no. 2, pp. 287–295, Feb. 1997.
[8] J. A. Encinar, "Design of two-layer printed reflectarrays using patches of variable size," *IEEE Trans. Antennas Propag.*, vol. 49, no. 10, pp. 1403–1410, Oct. 2001.
[9] M. E. Bialkowski and K. H. Sayidmarie, "Investigations into phase characteristics of a single-layer reflectarray employing patch or ring elements of variable size," *IEEE Trans. Antennas Propag.*, vol. 56, no. 11, pp. 3366–3372, Nov. 2008.
[10] R. Remski, "Analysis of PBG surfaces using Ansoft HFSS," *Microw. J.*, vol. 43, no. 9, pp. 190–198, Sept. 2000.
[11] K. H. Sayidmarie and M. E. Bialkowski, "Investigations into unit cells offering an increased phasing range for single-layer printed reflectarrays," *Microw. Opt. Technol. Lett.*, vol. 50, no. 4, pp. 1028–1032, Apr. 2008.
[12] H. Holma and A. Toskala, *WCDMA for UMTS: HSPA Evolution and LTE*, 4th ed. Hoboken, NJ: Wiley, 2007.